Beni-Suef University Journal of Basic and Applied Sciences

RESEARCH

Open Access

Integrated in vivo and in silico evaluation of sweet basil oil as a protective agent against cisplatin-induced neurotoxicity in mice

Doaa Shaaban Mohamed[1], Olfat Shehata[2*], Mai Mohamed Labib[3] and Nema Sayed Shaban[4]

Abstract

Background Cisplatin is a wide-ranging antineoplastic drug. Neurotoxicity is one of cisplatin's side effects that restrict its usage. This study aimed to investigate the possible protective properties of sweet basil oil against cisplatin-induced neurotoxicity in mice. A docking study was carried out to elucidate the fundamental mechanism of sweet basil oil's ameliorative influence. Thirty male mice were allocated into three groups as follows: control group, cisplatin group (2.3 mg/kg), and sweet basil oil group (25 µl/kg basil oil + cisplatin 2.3 mg/kg). Cisplatin was given for five successive days, followed by five days of rest, for two cycles, while sweet basil oil was orally administered for 21 successive days.

Results Our results revealed that sweet basil oil's antioxidant activity ameliorated the oxidative stress induced by cisplatin in mice's brains via lowering MDA levels and increasing CAT activity and Nrf_2 levels. Also, the anti-apoptotic activity of sweet basil oil was obvious via lowering the gene expression levels of Bid and caspase-3 but did not affect the serum level of P38 MAPK. Changes in acetylcholinesterase activity, serotonin and dopamine levels induced by cisplatin were significantly alleviated by sweet basil oil.

Conclusion Sweet basil oil can be used as a food supplement to guard against cisplatin-induced neurotoxicity.

Keywords Basil oil, Brain, Cisplatin, Apoptosis, Oxidative stress, Molecular docking

*Correspondence:
Olfat Shehata
Olfat_shehata@yahoo.com; olfat.magouda@vet.bsu.edu.eg
Full list of author information is available at the end of the article

Graphical abstract

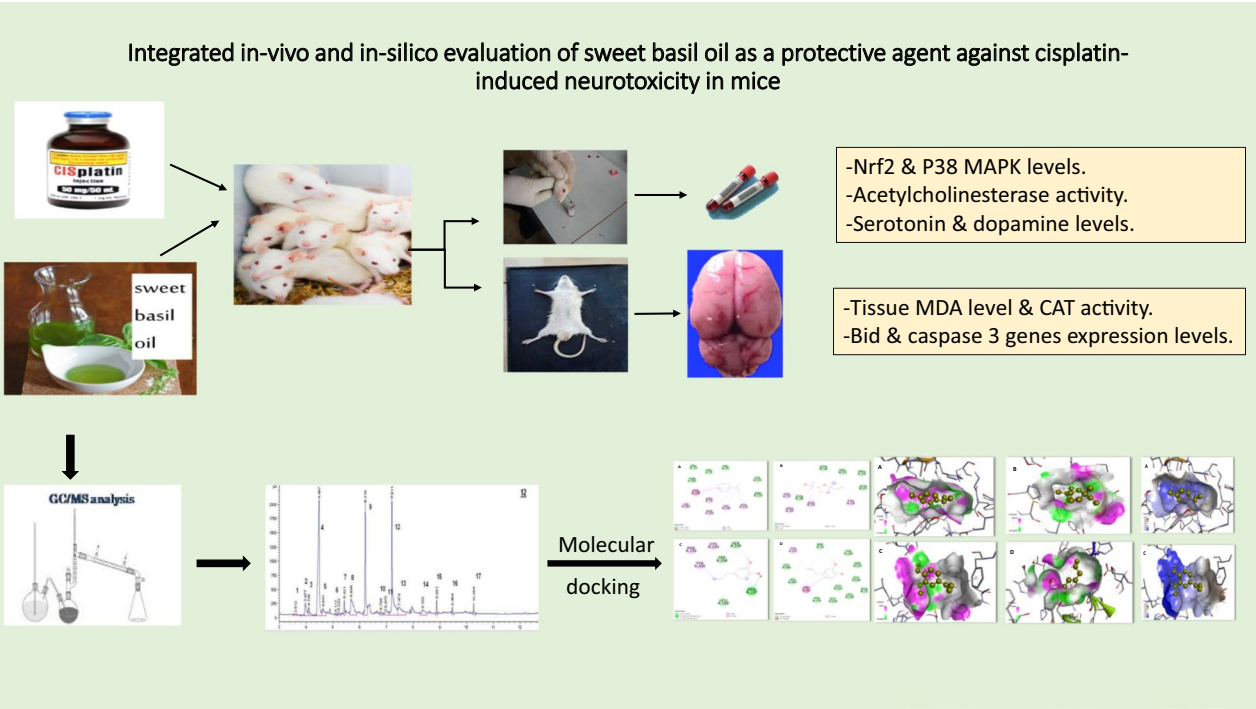

1 Background

Cisplatin, also known as cis-diamine, dichloroplatinum (II), is an anticancer medicine that is commonly used to treat tumors such as head and neck, as well as testicular, ovarian, brain and colon cancers [1]. Despite its efficacy, cisplatin has many serious side influences, involving neurotoxicity, nephrotoxicity, bone marrow toxicity, and ototoxicity [2].

In different organs of rats, cisplatin metabolism is correlated positively with specific glutathione *S*-transferase activities which determined the extent of cellular uptake or retention of cisplatin [3]. Several studies declared that cisplatin-induced cytotoxicity is closely related to increased ROS generation which alters the mitochondrial membrane potential (MMP) and damages the respiratory chain, subsequently triggering the apoptotic process [4]. Additionally, cisplatin rapidly accumulates in mitochondria and deteriorates the mitochondrial structure and metabolic function resulting in changes in the level of metabolites related to the tricarboxylic acid cycle and glycolysis pathway [5].

The most prevalent and dose-limiting consequence of cisplatin is neurotoxicity [6]. Many pathophysiological processes, including oxidative stress, inflammation, mitochondrial impairment, DNA destruction, and apoptosis in the nerve cell, have been hypothesized in previous research to explain the neurotoxicity associated with cisplatin-based treatment. According to the research, the brain is most susceptible to oxidative stress attributable to its high amount of polyunsaturated fatty acids (PUFAs), which are particularly vulnerable to reactive oxygen species (ROS) damage [7].

Cisplatin can pass the brain barrier and accumulate in the brain, increasing the production of ROS which intermingle with lipids, and DNA initiating lipid peroxidation and DNA damage [8]. Previous research has shown that cisplatin causes apoptosis via activating mitogen-activated protein kinase (MAPK) passageways throughout the formation of DNA and ROS cross-linking [9].

Much recent literature in alternative medicine have described the use of natural products to reduce the impact of xenobiotics [10]. As a result, there is a growing interest in using natural products and medicinal plants to discover new pharmacologically active compounds. Antioxidant supplementation has been shown in numerous studies to diminish the neurotoxic side effects of cisplatin, which work synergistically to boost anticancer

activity and diminish side effects [11]. *Ocimum basilicum L.*, commonly named sweet basil, is a popular herb belonging to the *Lamiaceae* family. Basil leaves have traditionally been used to remedy a diversity of ailments, involving cancer, convulsions, diarrhea, epilepsy, and bronchitis [12].

Basil oil contains physiologically active ingredients that have antioxidant and antibacterial activities, insecticidal, larvicidal, anticonvulsant, and anti-inflammatory properties. Many active components such as linalool, methyl cinnamate, methyl chavicol, and eugenol have been found in the chemical composition of basil oil, according to previous study [13]. This oil contains a variety of volatile compounds primarily terpenes and terpenoids(its oxygenated derivatives), and aliphatic and phenol-derived aromatic components [14]. Basil oil is a popular ingredient that is used in foodstuff, therapeutic and cosmetic industries. Basil's phenolic elements (linalool, lineol, limonene, estragole, eugenol, and geraniol) have economic value [15]. The acute toxicity of the essential oil of the cultivar "Maria Bonita" obtained from *Ocimum basilicum L.* in mice and the lethal dose causing 50% death (LD50) was 532 mg/kg body wt [16]. Several studies have shown that basil oil is safe and has potent antioxidant activity [17–20]. The purpose of the current study was to look into the antioxidant and neuroprotective properties of sweet basil oil to counter cisplatin-provoked neurotoxicity in mice by assessing oxidant/antioxidant pointers and apoptotic indicators in affected mice's brain tissues. In addition, molecular docking was done to gain insight into the binding mode of some sweet basil oil constituents (α-Pinene, gamma-terpinene, cis-linalool oxide, trans-linalool oxide, n-octanol, linalool, methyl chavicol, and eugenol), and catalase (CAT), Bid, caspase 3 and acetylcholinesterase.

2 Methods

2.1 Chemicals

Cisplatin vials (1 mg/ml) are obtained from El-Borg Pharmacy in Beni-Suef, Egypt. The sweet basil oil was given by the Harraz for Food Industry and Natural Products Co. in Cairo, Egypt. Commercial kits for malondialdehyde (MDA), catalase (CAT), and acetylcholinesterase were purchased from the Biodiagnostic Company, Cairo, Egypt. Ray Biotech, USA, supplied ELISA kits that are used to estimate the serum levels of P38 mitogen-activated protein kinase (P38 MAPK), nuclear factor erythroid 2-related factor 2 (Nrf_2), dopamine, and serotonin. Catalog numbers of dopamine, serotonin, P38 MAPK, and Nrf2 are MBS269234, GWB-D1BB69, EM1199, and MBS2516218, respectively.

2.2 Animals and treatments

Thirty male mice were fed a balanced diet and had unrestricted access to water. The mice were ten weeks old and came from a laboratory animal house in Beni-Suef, Egypt. Mice were kept at 25°C room temperature, and 45% relative humidity. All experimental methods were in agreement with the guidelines of the local Animal Care and Use Committee established at the Beni-Suef University (BSU-IACUC). The study was conducted after obtaining the approval number (022–315) to perform the animal experiments. The mice were randomly allocated into three groups (10 for each) one week following acclimatization:

Control group (C): Mice were intraperitoneally injected with 0.9% saline.

Cisplatin group (Cis): Cisplatin was obtained as vials ready for injection. Mice were intraperitoneally injected with cisplatin (2.3 mg/kg) for five successive days, followed by five days of rest, for two cycles [21].

Basil oil group (Bo): Animals were administered sweet basil oil orally using a stomach tube for 21 successive days at a dose of 25 µl/kg/day [22], and intraperitoneal injection of cisplatin (2.3 mg/kg) was given for 5 days, followed by 5 days of rest, for two cycles along with basil oil administration.

2.3 Sampling and biochemical analysis

Retro-orbital bleeding was employed to collect the blood samples 24 hours following the last dose, and blood samples were collected from each mouse. Clotted blood samples were centrifuged at 3000 rpm for 15 minutes to separate the serum. The sera were kept at −20°C until they were used.

Using light ether anesthesia, cervical dislocation was done. For removing the brain samples, decapitation of the mouse head, the skull was exposed by cutting the skin on top of the head, and flipping the skin all over the head to help hold the head and cutting the occipital and inter parietal bones. Then, following an incision in the skull along the sagittal and parietal sutures, a hole was made in the skull at the intersection between frontal and parietal bones, and the tip of the scissors was inserted to crack open the top part of the skull. The remaining skull was removed to fully reveal the brain. With forceps, the nerves and peduncles that were still connected to the brain were removed and flipped the brain out of the skull. The brain samples were quickly removed, and part of brain tissue were dissected, and immediately

flash-frozen in liquid nitrogen for RT-PCR. The rest of brain tissue was used for tissue homogenate for estimation of the oxidant/antioxidant indices.

2.3.1 Estimation of brain function biomarkers

The serum level of acetylcholinesterase was measured using a QuantiChrom™ acetylcholinesterase assay Kit. The Assay was based on an improved method [23], in which thiocholine produced by the action of acetylcholinesterase formed a yellow color with 5,5'-dithiobis (2-nitrobenzoic acid). The intensity of the product color, measured at 412 nm, is proportionate to the enzyme activity in the sample.

2.3.2 Oxidative/antioxidant indices

The concentration of MDA was measured according to [24] in which the malondialdehyde reacts with thiobarbituric acid (TBA) in an acidic medium at a temperature of 95 °C for 30 min creating a thiobarbituric acid reactive product. At 534 nm, the pink product's absorbance can be measured. The CAT assay was based on the reaction with methanol in the presence of an optimum concentration of H_2O_2, and the formaldehyde produced is detected colorimetrically with 4-amino-3-hydrazino-5-mercapto-1,2,4-triazole (purple) as the chromogen. When Purpald reacts with aldehydes, it particularly creates a bicyclic heterocycle that, when oxidized, turns purple and can be detected spectrophotometrically at 540 nm [25].

2.3.3 Determination of serum levels of serotonin, dopamine, Nrf_2, and P38 MAPK

The serum levels of serotonin, dopamine, Nrf_2, and P38 MAPK were assessed by ELISA according to the manufacturer's guidelines. The kit was based on a sandwich enzyme-linked immunosorbent assay technique. The micro-ELISA plate supplied in these kits has been pre-coated with a Mouse specific antibody to serotonin or dopamine or Nrf2 or P38 MAPK. Samples or standards are added to the wells and combined with the specific antibody. Then, a biotinylated detection of antibodies specific for Mouse serotonin or dopamine or Nrf2 or P38 MAPK and Avidin-Horseradish Peroxidase (HRP) conjugate was added to each microplate well and incubated. Free components were washed away. The substrate solution was added to each well. Only those wells that contain Mouse serotonin or dopamine or Nrf2 or P38 MAPK, biotinylated detection antibody, and Avidin-HRP conjugated and appeared blue. The enzyme–substrate reaction was ended by stop solution addition and the color turned yellow. The optical density (OD) was measured spectrophotometrically at a wavelength of 450 nm ± 2 nm. Calculate the concentration of each parameter in the samples by comparing the OD of the samples to the standard curve.

2.3.4 Detection of bid and caspase 3 gene expression levels by real-time polymerase chain reaction (RT-PCR)

RNeasy Mini kit was used to extract total RNA (QIAGEN, CA, USA). Following the manufacturer's instructions, reverse transcription was carried out using the Superscript kit (Life Technologies, CA, USA). By following the manufacturer's instructions, qRT-PCR was used to measure the mRNA expression levels of Bid and caspase-3 by utilizing iTaq TM Universal SYBR Green Supermix reagents (BIO-RAD Laboratories, CA, USA).

For cDNA synthesis, an oligonucleotide (dT) 18 primers were used to reverse transcribe 5 µg of RNA and denature at 70 °C for 2 min. Denatured RNA was added to the reverse transcription mixture on ice. The tube was held at 42 °C for 1 h and next heated to 92 °C to stop the reaction. For quantitative RT-PCR, first-strand cDNA (5 µl) was used as indicated in Table 1 in a total volume of 25 µl containing 12.5 µl of 2×SYBR Green PCR Master Mix and 200 ng of each primer. PCR reactions were performed on the Step One plus RT-PCR system. Data were evaluated using the ABI Prism 7500 Sequence Recognition System software. PE Biosystems sequence recognition software v1.7 was used for quantification. A comparative threshold cycle approach was used to calculate the relative expression of the interrogated genes. The β-actin gene was used to normalize these data. All these processes were performed according to the procedure defined by [26].

Table 1 The primer sequences used for amplification of mRNAs encoding Bid and caspase 3 genes

mRNA	Sequences (5` → 3`)	Accession no
Bid	Forward primer: AAGAAGGTGGCCAGTCACAC	NC_000072
	Reverse primer: GTCCATCCCATTTCTGGCTA	
Caspase 3	Forward primer: CCTCAGAGAGACATTCATGG	NC_000074
	Reverse primer: GCAGTAGTCGCCTCTGAAGA	
β-actin	Forward primer: ATGAGCCCCAGCCTTCTCCAT	NC_000071
	Reverse primer: CCAGCCGAGCCACATCGCTC	

2.4 Phytochemical analysis of sweet basil oil

The chemical composition of the sweet basil oil sample was achieved using Trace GC-ISQ mass spectrometer with a direct capillary column. The temperature of the column oven was held at 50 °C at first and then, increased by 5 °C /min for 2 min reached the final temperature of 300 °C and held for 2 min. The temperature of the injector and MS transfer line was held at 270, 260 °C, respectively. At a constant flow rate of 1 ml/min, Helium was used as a carrier gas. The solvent delay was 4 min, and diluted samples of 1 µl were injected automatically. EI mass spectra were gathered at 70 eV ionization voltages over the scale of m/z 50–650 in full scan mode. The ion source temperature was set at 200 °C. The constituents were recognized by comparison of their retention times and mass spectra with those of WILEY 09 and NIST 14 mass spectral database [27].

2.5 Molecular docking

Molecular docking was performed for catalase, Bid, caspase-3, and acetylcholinesterase against eight components: Gamma-terpinene, Methyl Chavicol, Cis-linalool oxide, Eugenol, Linalool, Trans-linalool oxide, α – Pinene, and Noctanol. Initially, the biological data and 3D structure of each enzyme were collected from UniProtKB (ID: P24270, P70444, P70677, P21836) databases for catalase, Bid, caspase-3, and acetylcholinesterase, respectively. We obtained the structure of each component using the PubChem database [28]. For the energy minimization process, the alteration was done for all constituents by Swiss PDB Viewer software [29]. The format was changed from PDB to pdbqt by Open Babel software (version 2.3.1) [30]. Each enzyme and component was modified by adding hydrogen atoms to protein and ligand, and metals were treated using the Discovery Studio software (version 2019) [31]. Auto Dock Vina (Version 2.0) was used define the grid box with 1.00 Å spacing and a grid map of 78 94 82 XYZ Å points for catalase, 46 48 44 XYZ Å points for Bid, 76 56 82 XYZ Å points for caspase-3, and 72 58 84 XYZ Å points for acetylcholinesterase enzyme [32]. Van der Waals interactions, binding energy, and inhibition constant were ranked by Auto Dock [33]. Play molecule database was used to predict the interactions between the superior ligand and different pathways.

2.6 Statistical examination

Results were analyzed using SPSS software. One-way analysis of variance (ANOVA) and comparisons were carried out using the Tukey post hoc test. The data were exhibited as the mean with standard error (SE) was used to express data. The differences were considered statistically significant at $p \leq 0.05$.

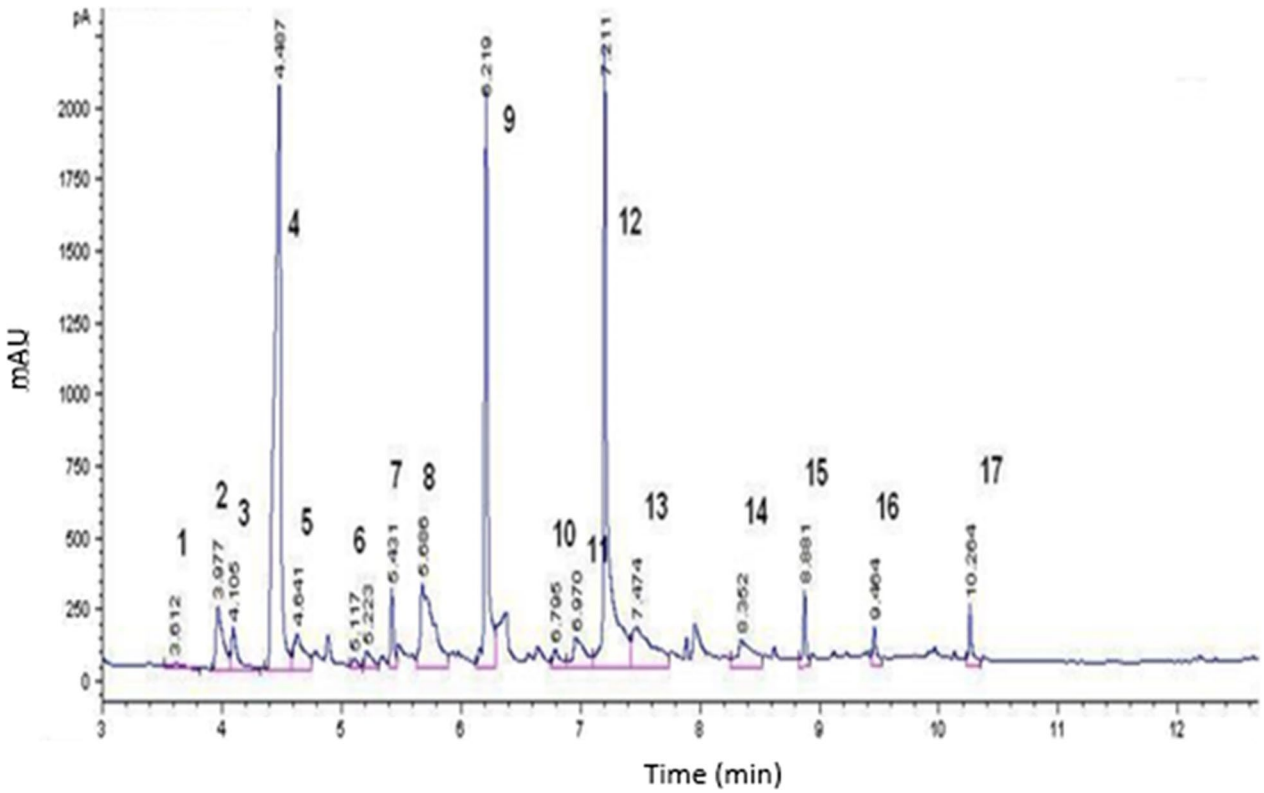

Fig. 1 Area percent level of chemical constituents of sweet basil oil

Table 2 The phytochemical analysis of sweet basil oil using gas chromatography-mass spectrometry

Peak NO	Component name	RT (retention time)	Area %
1	Not identify	3.612	T
2	α—Pinene	3.977	6.562
3	Sabinene	4.105	4.442
4	1,8-cineole	4.487	25.581
5	Gamma-terpinene	4.641	5.064
6	Cis-linalool oxide	5.223	1.67
7	Trans-linalool oxide	5.431	1.407
8	n-octanol	5.686	6.597
9	Linalool	6.210	12.211
10	Neo-allo-ocimene	6.795	0.79
11	Cis-menth-2-en-1-ol	6.970	4.121
12	Methyl Chavicol	7.211	18.95
13	Isocarveol -dehydro	7.474	6.742
14	β-cycloelemene	8.352	2.473
15	Eugenol	8.881	1.282
16	α—Copaene	9.464	0.882
17	β -Elemene	10.264	1.226

3 Results

3.1 Phytochemical analysis

The results of the phytochemical analysis of sweet basil oil and the area percent level of its chemical constituents of it are shown in Fig. 1 and Table 2.

3.2 Changes in oxidative/antioxidant indices

The present data showed that cisplatin diminished the antioxidant capacity of mice brain tissue as noticed by a statistically significant increase in MDA level ($p \leq 0.001$) and a statistically significant decrease in catalase enzyme activity ($p \leq 0.001$) as well as a statistically significant increase in Nrf_2 serum level ($p \leq 0.001$) in Cis group when compared to the control group. In the basil group, there was a statistically significant decrease in MDA ($p \leq 0.01$) and a statistically significant decrease in CAT ($p \leq 0.05$) and Nrf2 ($p \leq 0.001$) when compared to control group. Co-administration with sweet basil oil noticeably offsets the cisplatin-provoked oxidative stress via a statistically significant decrease in MDA ($p \leq 0.001$) and a statistically significant increase in CAT and Nrf_2 ($p \leq 0.05$) as compared to Cis group as shown in Table 3.

Table 3 Changes in brain tissue levels of CAT, MDA and serum level of Nrf2 in various experimental groups

	CAT U/g	MDA nmol/g	Nrf2 ng/ml
C group	1.57 ± 0.07^{a}	1.15 ± 0.04^{a}	1.88 ± 0.05^{a}
Cis group	0.87 ± 0.5^{b}	2.69 ± 0.09^{b}	2.99 ± 0.06^{b}
Bo group	1.28 ± 0.05^{c}	1.84 ± 0.08^{c}	2.63 ± 0.08^{c}

Values are exemplified as mean ± mean standard error. The dissimilar superscript letters denote a noteworthy difference at ($p \leq 0.05$) between various groups in the same column

3.3 Changes of pro-apoptotic parameters

In the current study, Bid and caspase-3 gene expression levels were significantly ($p \leq 0.001$) increased in the brain tissue of the Cis group in comparison with the control group. However, the administration of sweet basil oil significantly ($p \leq 0.001$) downregulated this expression when compared to the cisplatin group. The expression of Bid ($p \leq 0.001$) and caspase-3 ($p \leq 0.01$) genes was significantly decreased in the basil oil group in comparison with the control group as shown in Fig. 2. There was a statistically significant decrease in P38 MAPK serum level in both Cis ($p \leq 0.01$) and Bo ($p \leq 0.05$) groups as compared to the control, and no statistically significant changes were noticed between Cis and Bo groups (Fig. 3).

3.4 Changes in brain function biomarkers

The data presented in Fig. 4 showed that cisplatin significantly increased the serum levels of acetylcholinesterase ($p \leq 0.001$) and dopamine ($p \leq 0.001$) and significantly decreased the serum level of serotonin ($p \leq 0.01$) in comparison with the control group. Administration of sweet basil oil significantly ($p \leq 0.01$) ameliorates this effect as compared to the Cis group.

3.5 Molecular docking results

The use of computer simulation to visualize molecular structure modeling and docking is a promising method [34]. The in silico docking technique facilitates the comprehension of the chemical and topological properties of the enzyme binding site and the basis for recognizing the enzyme and its docked components [35]. Table 4 illustrated the binding affinity results for all the docked components-complexes, while Table 5 illustrated the superior docked-components for each enzyme and it's H-bond and hydrophobicity residues. The 2D chemical interactions, which ranged from conventional hydrogen bond, pi-donor hydrogen bond, alkyl, pi-alkyl, van der Waals, and pi-sigma, are demonstrated in Fig. 5 for the superior docked component. Also, the hydrophobicity area in brown color and H-bond as a donor in pink color and acceptor in green color are illustrated in Figs 6 and 7. Finally, the solvent accessible surface (SAS) for each superior docked complex is investigated in Fig. 8. The heatmap illustrated the interaction probability between the superior three docked components and different pathways (Fig. 9).

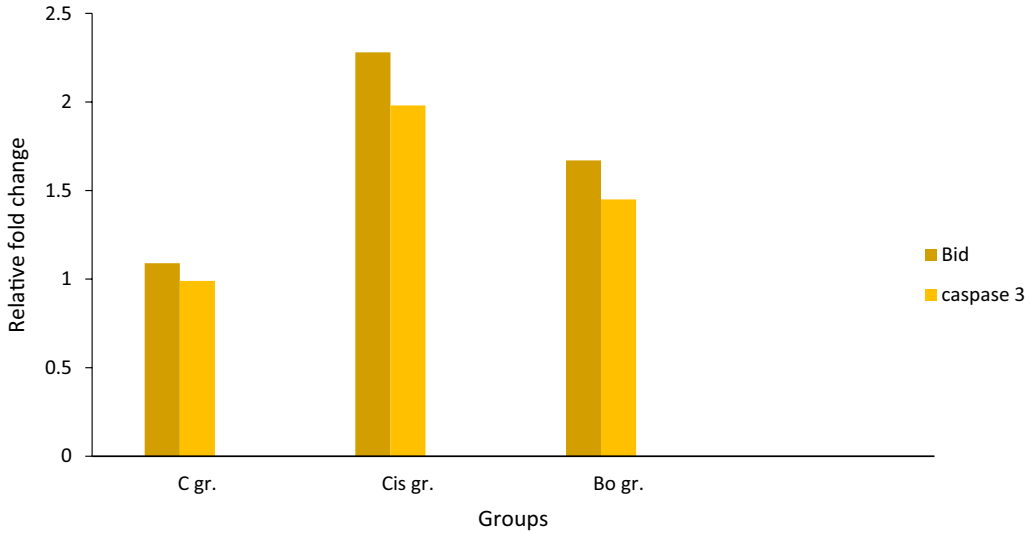

Fig. 2 Relative expression levels of Bid and Caspase 3 genes in different groups. The dissimilar superscript letters denote a noteworthy difference at ($p \leq 0.05$)between various groups. Values are represented as mean ± standard error of mean. C gr: control group, Cis gr:cisplatin group, BO gr: sweet basil oil group.

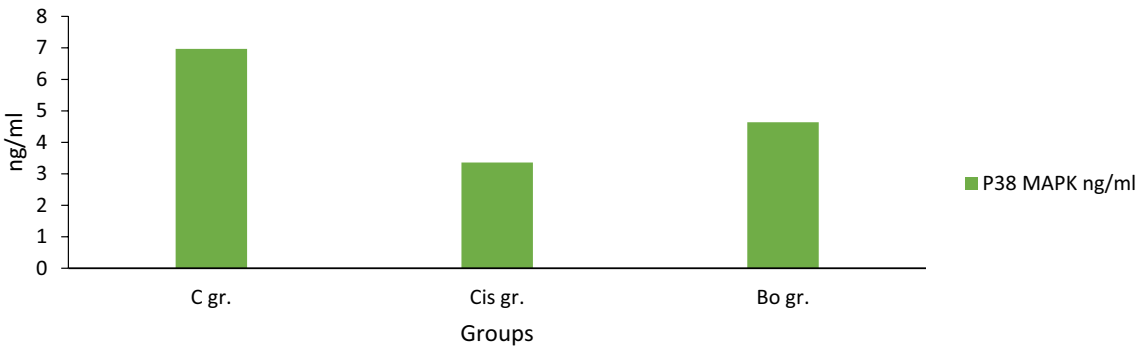

Fig. 3 Changes in serum level of P38 MAPK in different groups. The dissimilar superscript letters denote a noteworthy difference at ($p \leq 0.05$) between various groups. Values are represented as mean ± standard error of mean. C gr: control group, Cis gr: cisplatin group, BO gr: sweet basil oil group.

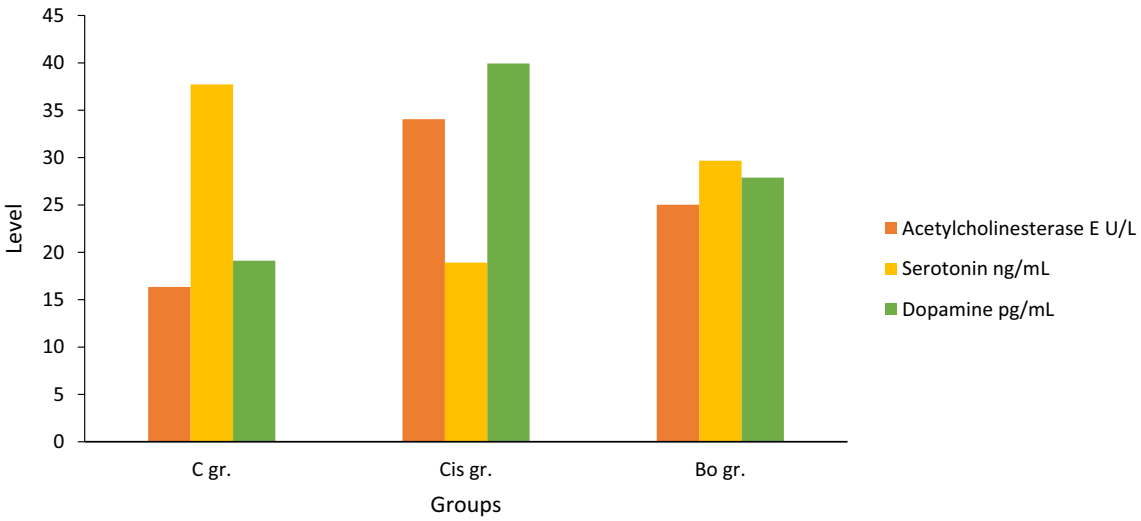

Fig. 4 Changes in brain function biomarkers in different groups. The dissimilar superscript letters denote a noteworthy difference at ($p \leq 0.05$) between various groups. Values are represented as mean ± standard error of mean. C gr: control group, Cis gr:cisplatin group, BO gr: sweet basil oil group.

Table 4 The total docking binding energy score for each docked enzyme-ligand complex

	Name of ligand	Binding energy (kcal/mol)
Catalase	Gamma-terpinene	−6.6
	Methyl Chavicol	−6.2
	Cis-linalool oxide	−6.2
	Eugenol	−6.1
	Linalool	−6.1
	Trans-linalool oxide	−5.7
	α – Pinene	−5.5
	Noctanol	−4.9
Bid	Cis-linalool oxide	−5.2
	Eugenol	−5
	α – Pinene	−5
	Gamma-terpinene	−5
	Trans-linalooloxide	−4.9
	Methyl Chavicol	−4.8
	Linalool	−4.7
	Noctanol	−4.1
Caspase-3	Eugenol	−5.2
	Gamma-terpinene	−5.2
	Methyl Chavicol	−5
	α – Pinene	−5
	Cis-linalool oxide	−4.9
	Trans-linalool oxide	−4.9
	Linalool	−4.5
	Noctanol	−4.1
Acetylcholinesterase	Eugenol	−6.6
	Gamma-terpinene	−6.5
	α – Pinene	−6.3
	Cis-linalool oxide	−6.2
	Trans-linalool oxide	−6.1
	Methyl Chavicol	−5.9
	Linalool	−5.6
	Noctanol	−5

4 Discussion

The significant incidence of cisplatin side effects affects its clinical outcomes [36] necessitating dosage adjustment or discontinuation of the regimen [37]. The goal of this study was to see if basil oil has any neuroprotective properties against cisplatin-induced neurotoxicity. The major processes in the physiopathology of chemotherapy are oxidative stress and, as a result, neuronal damage [38] in line with our results which revealed a marked increase in the level of MDA parallel to the reduction in the CAT activity in the brain of mice given cisplatin alone [39] reported that due to cisplatin's high reactivity, it exacerbated oxidative stress in tissues, depleted glutathione, and inhibited the activity of the antioxidant enzymes resulting in the accumulation of ROS inside the cells. The antioxidant activity of Nrf_2 helped to reduce oxidative stress [40], and it has been promoted in the hopes of shielding against oxidative stress [41]. In the current study, the serum level of Nrf_2 in mice treated with cisplatin was significantly increased in agreement with [42] who mentioned that the Nrf_2 pathway may be activated to repel oxidative stress and exert a cytoprotective impact to lessen oxidative stress. In the current study, co-administration of sweet basil oil with cisplatin significantly ameliorated oxidative/antioxidants alterations induced by cisplatin in the same line with a previous study revealed that sweet basil oil inhibited lipid peroxidation and raised the activities of superoxide dismutase, glutathione peroxidase, and catalase enzymes, implying a role for sweet basil oil in free radical scavenging [43, 44] mentioned that because of the reactive oxygen species scavenging activity of phenolic, flavonoids, and tannin contents, sweet basil oil has a neuroprotective impact, as it reduced the size of cerebral infarct and lipid peroxidation in the brain.

In the current study, cisplatin-induced apoptosis in brain tissue where Bid and caspase-3 gene expression levels, pro-apoptotic genes, were considerably

Table 5 The superior docking complex for each domain, binding energy, hydrophobic residues, and H-bond

Name of complex	Binding energy (kcal/mol)	Hydrophobic residues	H-bond
Catalase-Gamma-terpinene	−6.6	TYR A: 358, ALA A: 133, ARG A: 72, VAL A: 146, ARG A: 112, HIS A: 75, PHE A: 334, HIS A: 362	–
Bid-Cis-linalool oxide	−5.2	TYR A: 19	–
Caspase-3-Eugenol	−5.2	ARG A: 207, TYR A: 204, PHE A: 256	ARG A: 207, SER A: 65
Acetylcholinesterase-Eugenol	−6.6	TRP A: 86, TYR A: 337	–

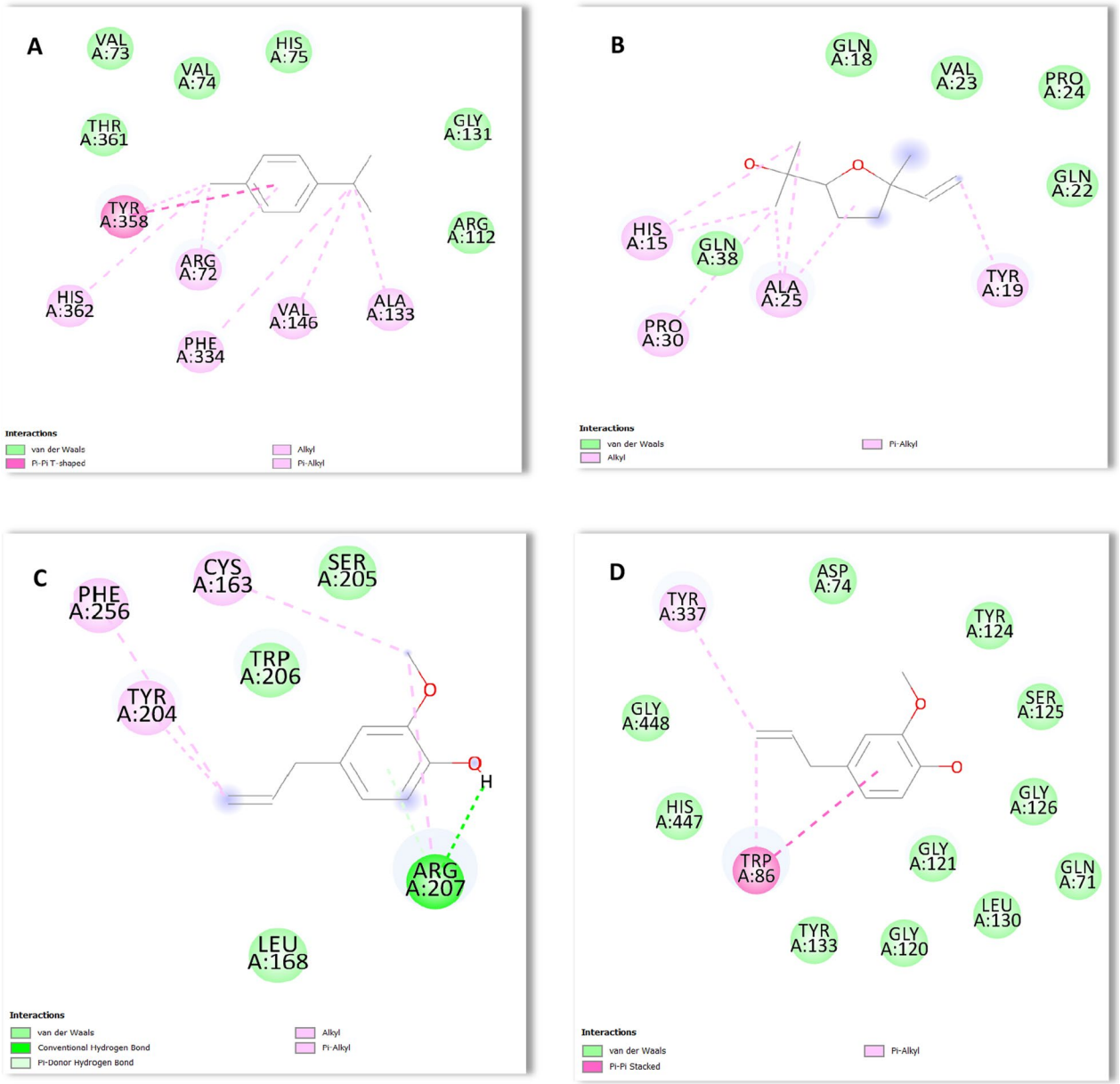

Fig. 5 The 2D chemical interactions of the docked complexes with: **A** Catalase-Gamma-terpinene, **B** Bid-Cis-linalool oxide, **C** Caspase-3-Eugenol, **D** Acetylcholinesterase-Eugenol

increased in comparison with the control group. These results are in good agreement with [45] who explained that cisplatin injection gives the pro-apoptotic mediators the upper hand because it stimulates the movement of Bax into mitochondria, resulting in the liberation of cytochrome c into the cytoplasm and consequent activation of caspase-3, which in turn motivates the other caspase enzymes, initiating apoptosis and the fragmentation of DNA and protein in cells. MAPKs are a structurally related family of serine/threonine protein kinases that regulate essential biological functions such as cell growth and survival by synchronizing a diversity of extracellular signaling paths. Inactivation of this system either helps to or inhibits apoptosis induced by cisplatin; hence, targeting these signaling pathways is controversial [46]. In our study, the serum level of p38 MAPK significantly declined in the cisplatin group in harmony with [47] who informed that inactivation of the p38 MAPK path caused an increase in ROS and caused apoptosis. Moreover, [48] documented that in renal tubule epithelial cell lines, p38

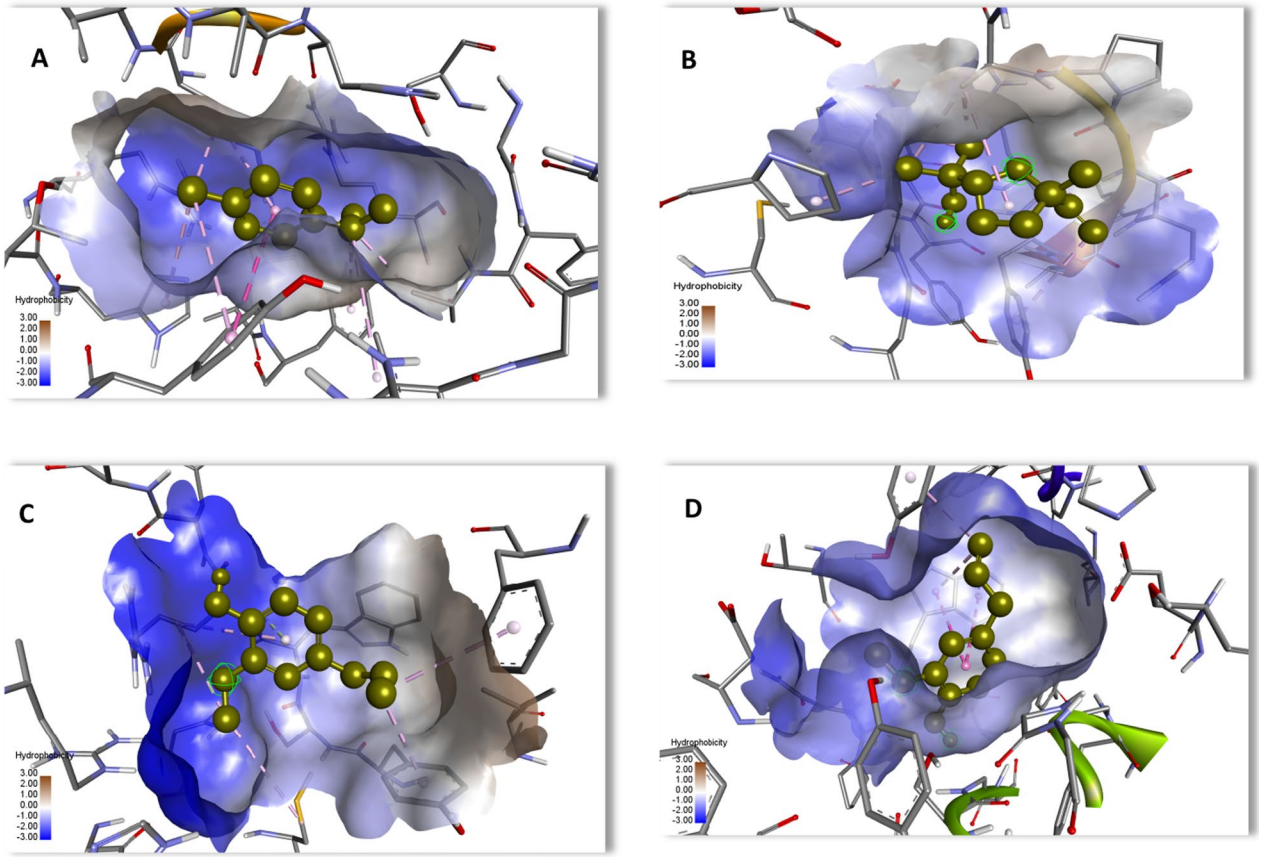

Fig. 6 The hydrophobicity of the docked complexes with: **A** Catalase-Gamma-terpinene, **B** Bid- Cis-linalool oxide, **C** Caspase-3-Eugenol, **D** Acetylcholinesterase-Eugenol

MAPK inactivation stimulates cisplatin-induced cell death via glutathione exhaustion. On the other hand, our results revealed that sweet basil oil has an anti-apoptotic upshot as it significantly diminished the gene expression levels of Bid & caspase-3 in the brain tissue, but it did not affect P38 MAPK serum level. Ayuob et al. [49] confirmed our results as they mentioned that in the hippocampus of mice, sweet basil oil significantly reduced caspase-3 expression and apoptotic nerve cells. Because apoptosis is well recognized to be one of the foundations of cisplatin-provoked toxicity via numerous pathological incentives, including oxidative stress [50], we assumed that sweet basil oil's protective effect against cisplatin-induced toxicity is referred to its antioxidant activity as it is a significant source of phenolic compounds which trap singlet and triplet oxygen and degrade peroxides [51]. In the present study, the noticeable elevation in the acetylcholinesterase activity observed in cisplatin-treated mice was in line with [52]. However, a marked reduction in acetylcholinesterase activity in sweet basil oil-treated mice suggests that sweet basil oil may play a protective function in cisplatin-induced neurotoxicity in accordance with [53] who reported that eugenol, the major ingredient of basil oil, was found to have substantial anti-acetylcholinesterase activity when tested separately. Our findings revealed that cisplatin significantly lessened the serum level of serotonin and raised the serum level of dopamine in line with a previous study indicating that various neurotransmitter systems are affected as a result of chemotherapy [54]. The changes in the serum levels of serotonin and dopamine neurotransmitters induced by cisplatin were alleviated by sweet basil oil co-administration in agreement with [55]. Caryophyllene, humulene, 1,8-cineole, linalool, and camphor are some of the sweet basil oil components that have been found to have anxiolytic and sedative properties [56].

In general, it was interesting to predict the scenes of protein–ligand interactions, whether they were activation or inhibition interactions at the level of enzymes, especially in the region of the active site. The use of molecular docking to visualize each interaction between enzymes and compounds is a promising method. Expecting chemical interactions could smooth the understanding of the overview with each detail about the effect of sweet basil

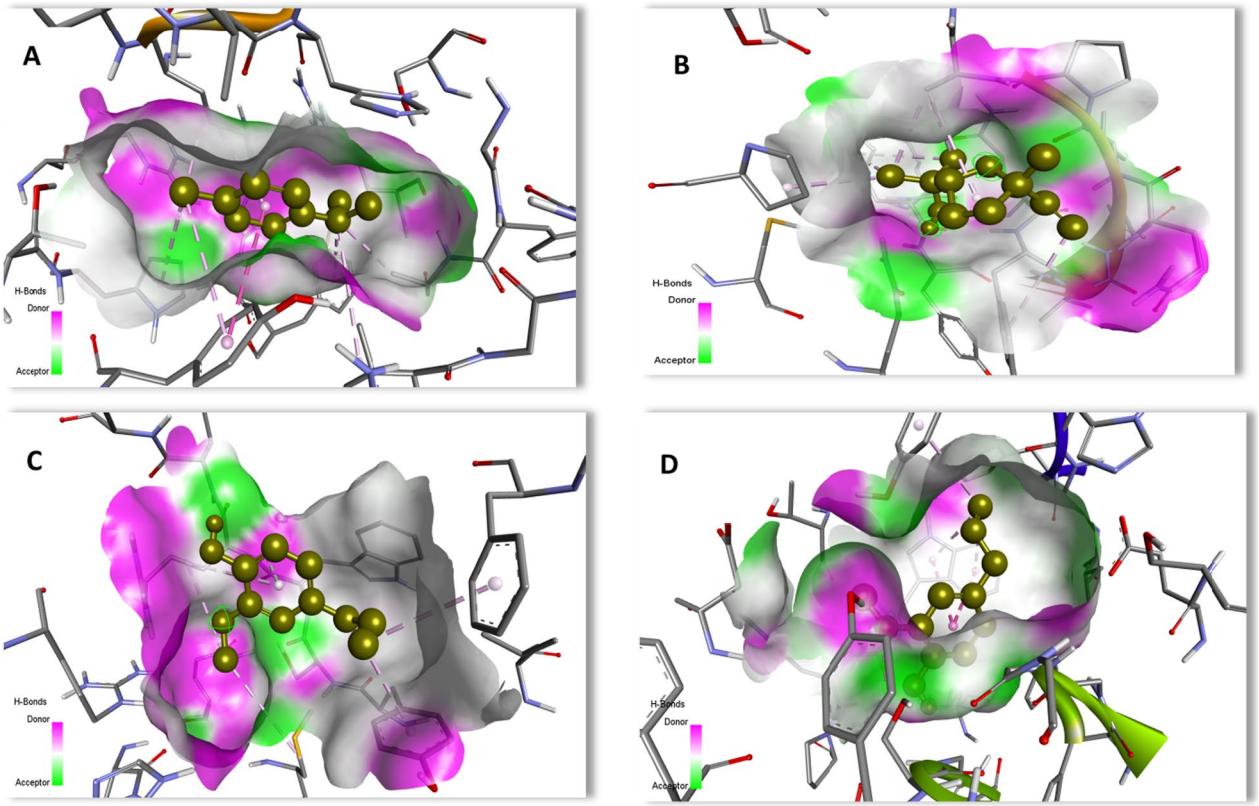

Fig. 7 The H-bond of the docked complexes with: **A** Catalase-Gamma-terpinene, **B** Bid- Cis-linalool oxide, , **C** Caspase-3- Eugenol, **D** Acetylcholinesterase- Eugenol.

oil as a protective agent against cisplatin-induced neurotoxicity in mice. Beginning with the best binding energy: Catalase-Gamma-terpinene, Bid-Cis-linalool oxide, Caspase-3- Eugenol, and Acetylcholinesterase-Eugenol docked complexes were the best among the constituents of sweet basil oil, with the lowest binding energy of −6.6, −5.2, −5.2, and −6.6, respectively. Lower binding energy was thought to be closer to the complex's natural state in the molecular docking predicted complex [57]. After that, the 2D chemical interactions clarified that Caspase-3-Eugenol docked complex profit the most substantial chemical interactions with one conventional hydrogen bond and one pi-donor hydrogen bond located in the amino acid ARG A: 207. Other docked complexes obtained some chemical interactions like alkyl, pi-alkyl, pi-sigma, and van der Waals. Through the hydrophobicity results in a table (5), the catalase-gamma-terpinene complex obtained eight hydrophobic residues, while bid-cis-linalool oxide complex obtained one, caspase-3-eugenol obtained three, and acetylcholinesterase-eugenol complex obtained two. It was well known that H-bonds govern molecular interactions through a previously unknown donor–acceptor coupling mechanism that reduces rivalry with water [58]. The most interactive donors (pink color) and acceptors (green color) were illustrated in the Catalase-Gamma-terpinene complex (Fig. 6). Finally, the eight natural components extracted from sweet basil oil proved their ability to interact with each domain, especially Gamma-terpinene, Cis-linalool oxide, and Eugenol. Caspase-3-Eugenol illustrated its ability to interact with two H-bonds, lower binding energy, and obtained several hydrophobic residues. The heatmap revealed that the Gamma-terpinene, Cis-linalool oxide, Eugenol, and cisplatin appeared to not be interacted with the different pathways.

5 Conclusions

In conclusion, in vivo and in silico findings revealed that sweet basil oil has the possible capability to improve cisplatin-induced neurotoxicity owing to its antioxidant and anti-apoptotic properties which are ascribed to radical scavenging actions of its constituents. Consequently, we recommended the consumption of sweet basil oil which can be considered a promising natural compound to counteract brain toxicity caused by cisplatin.

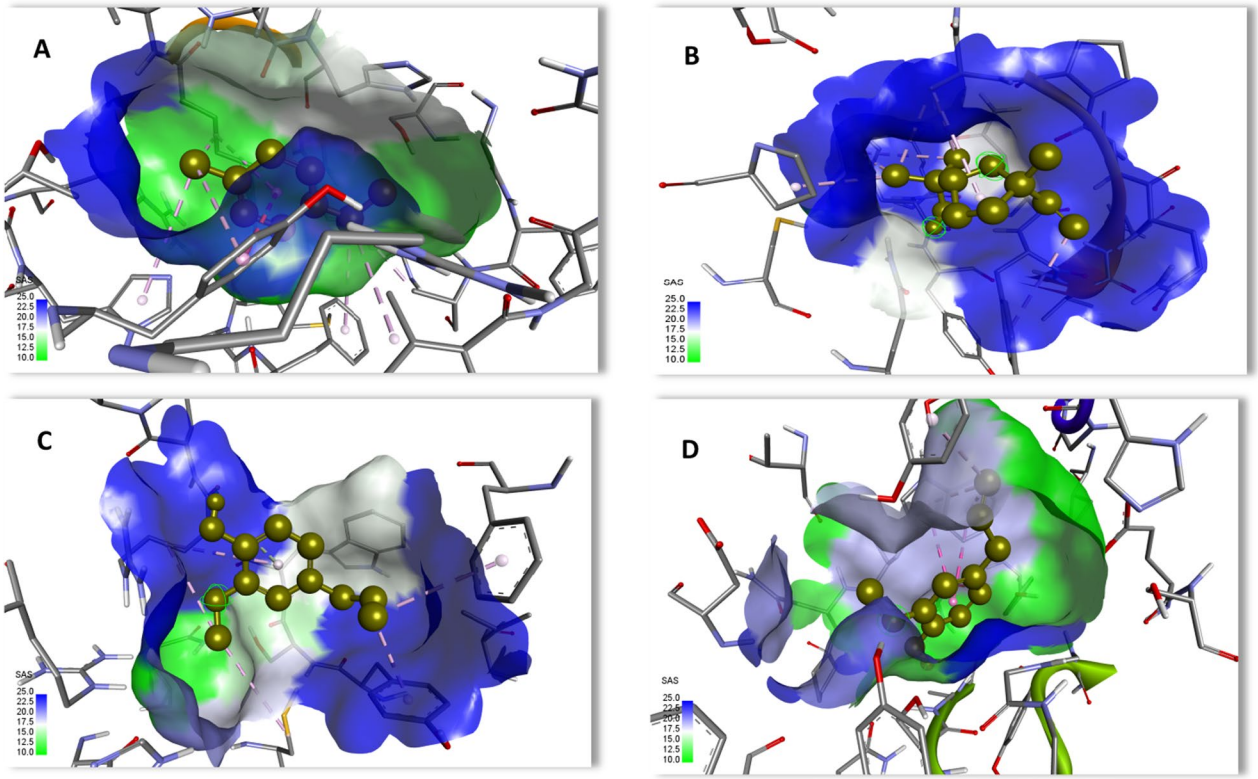

Fig. 8 SASA of the docked complexes with: **A** Catalase-Gamma-terpinene, **B** Bid- Cis-linalool oxide, **C** Caspase-3-Eugenol, **D** Acetylcholinesterase-Eugenol

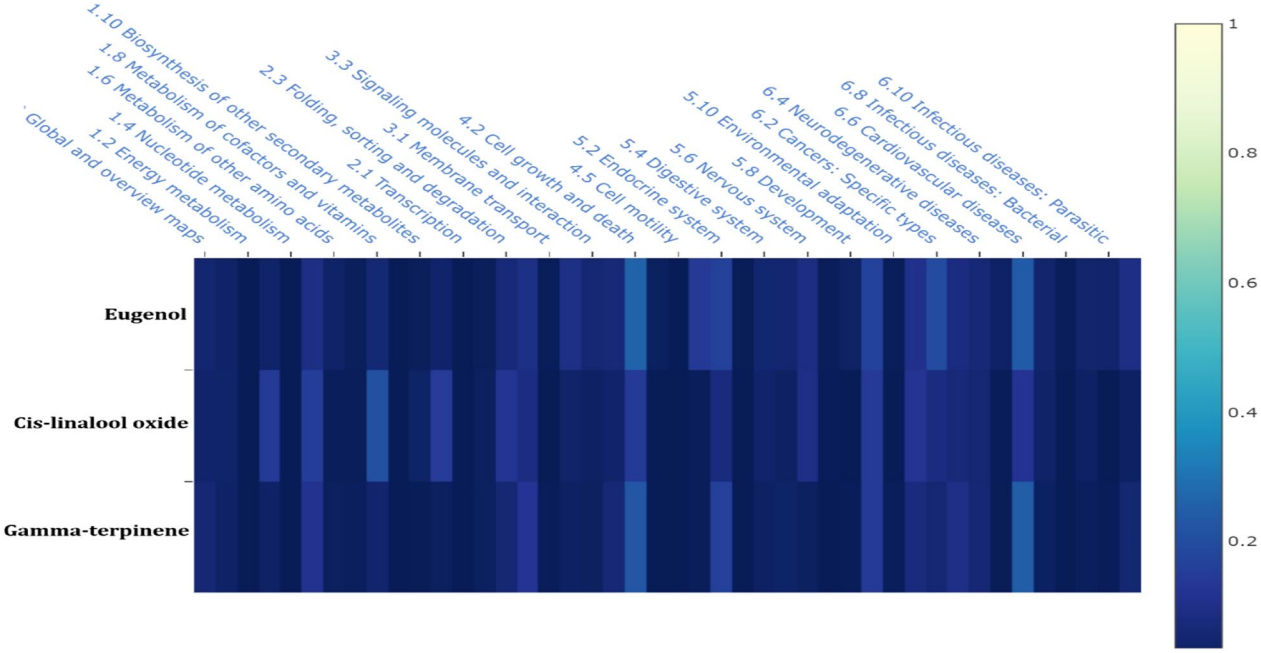

Fig. 9 A heatmap for the superior three components which illustrated the lowest interactions probabilities with the dark blue color between them and different pathways

Abbreviations

ROS	Reactive oxygen species
MAPK	Mitogen-activated protein kinase
CAT	Catalase
MDA	Malondialdehyde
Nrf2	Nuclear factor erythroid 2-related factor 2
PUFAs	Polyunsaturated fatty acids
SASA	The solvent accessible surface area
H-bond	Hydrogen bond

Acknowledgements
Not applicable.

Author contributions
DSM is the investigator, analyzed the results, and paper writing modeling and optimization. OSM contributed to supervision, contributed in performance of the experimental and laboratory work, reviewing and final editing, modeling and optimization. MML performing the molecular docking study, modeling and optimization. NSS contributed to conceptualization, performance of the experimental and laboratory work, reviewing and final editing, modeling and optimization. All authors have read and approved the manuscript.

Funding
There has been no funding for this study.

Availability of data and materials
All data generated or analyzed during this study are included in this published article.

Declarations

Ethical approval and consent to participate
All study measures were carried out consistent with the Research Ethical Committee of Beni-Suef University's Faculty of Veterinary Medicine with an approval number (022–315) to conduct the animal experiments.

Consent for publication
All authors who contribute to this manuscript confirm their consent for the publication of all data included in this manuscript.

Competing interests
The authors state that they have no competing interests.

Author details
[1]Department of Biochemistry and Chemistry of Nutrition, Faculty of Veterinary Medicine, Beni-Suef University, Beni-Suef 62511, Egypt. [2]Department of Clinical Pathology, Faculty of Veterinary Medicine, Beni-Suef University, Beni-Suef 62511, Egypt. [3]Department of Bioinformatics and Computer Networks, Agriculture Genetic Engineering Research Institute (AGERI), Cairo, Egypt. [4]Department of Pharmacology, Faculty of Veterinary Medicine, Beni-Suef University, Beni-Suef 62511, Egypt.

Received: 6 March 2023 Accepted: 18 June 2023
Published online: 15 July 2023

References

1. Podratz JL, Knight AM, Ta LE, Staff NP, Gass JM, Genelin K, Schlattau A, Lathroum L, Windebank AJ (2011) Cisplatin induced mitochondrial DNA damage in dorsal root ganglion neurons. Neurobiol Dis 41:661–668. https://doi.org/10.1016/j.nbd.2010.11.017
2. Paksoy M, Ayduran E, Sanlı A, Eken M, Aydın S, Oktay ZA (2011) The protective effects of intratympanic dexamethasone and vitamin E on cisplatin-induced ototoxicity are demonstrated in rats. Med Oncol 28:615–621. https://doi.org/10.1007/s12032-010-9477-4
3. Agar R, Khan AR, Poonia A (2015) Metabolism of cisplatin in the organs of Rattusnorvegicus: role of Glutathione S-transferase P1. Eur J Drug Metab-Pharmacokinet 40:45–51. https://doi.org/10.1007/s13318-014-0176-y
4. Valko M, Rhodes CJ, Moncol J, Izakovic M, Mazur M (2006) Free radicals, metals and antioxidants in oxidative stress-induced cancer. ChemBiol Interact 160:1–40
5. Alborzinia H, Can S, Holenya P, Scholl C, Lederer E, Kitanovic I (2011) Real-time monitoring of cisplatin-induced cell death. PLoS ONE 6:e19714
6. Bobylev I, Joshi AR, Barham M, Neiss WF, Lehmann HC (2018) Depletion of mitofusin-2 causes mitochondrial damage in cisplatin-induced neuropathy. MolNeurobiol 55:1227–1235. https://doi.org/10.1007/s12035-016-0364-7
7. Cui K, Luo X, Xu K, VenMurthy MR (2004) Role of oxidative stress in neurodegeneration: recent developments in assay methods for oxidative stress and nutraceutical antioxidants. Prog Neuropsychopharmacol Biol Psychiatry 28:771–99. https://doi.org/10.1016/j.pnpbp.2004.05.023
8. Aydin B, Unsal M, Sekeroglu ZA, Gülbahar Y (2011) The antioxidant and antigenotoxic effects of Pycnogenol® on rats treated with cisplatin. Biol Trace Elem Res 142:638–650. https://doi.org/10.1007/s12011-010-8781-3
9. Winograd-Katz SE, Levitzki A (2006) Cisplatin induces PKB/Akt activation and p38(MAPK) phosphorylation of the EGF receptor. Oncogene 25(56):7381–90. https://doi.org/10.1038/sj.onc.1209737
10. Khalil SR, Salem HFA, Metwally MMM, Emad RM, Elbohi KM, Ali SA (2020) Protective effect of Spirulina platensis against physiological, ultrastructural and cell proliferation damage induced by furan in kidney and liver of rat. Ecotoxicol Environ Saf 192:110256. https://doi.org/10.1016/j.ecoenv.2020.110256
11. Turan MI, Cayir A, Cetin N, Suleyman H, SiltelioğluTI TH (2014) An investigation of the effect of thiamine pyrophosphate on cisplatin-induced oxidative stress and DNA damage in rat brain tissue compared with thiamine: thiamine and thiamine pyrophosphate effects on cisplatin neurotoxicity. Hum Exp Toxicol 33:14–21. https://doi.org/10.1177/0960327113485251
12. Khalid KA, Hendawy SF, El-Gezawy E (2006) Ocimumbasilicum L production under organic farming. Res J Agric Biol Sci 2(1):25–32
13. Simon JE, Morales MR, Phippen WB, Vieira RF, Hao Z (1999) Basil: a source of aroma compounds and a popular culinary and ornamental herb. New Crops New Uses 16:499–505
14. Janick J, Simon JE (eds) (1990) In advances in new crops. Timber Press, Portland, pp 484–489
15. Sifola MI, Barbieri GG (2006) Yield and essential oil content of three cultivars of basil grown under different levels of nitrogen in the field. SciHortic 108:408–413. https://doi.org/10.1016/j.scienta.2006.02.002
16. Venâncio AM, Onofre ASC, Lira AF, Alves PB, Blank AF, Antoniolli AR, de Araujo BS (2011) Chemical composition, acute toxicity, and antinociceptive activity of the essential oil of a plant breeding cultivar of basil (Ocimumbasilicum L.). Planta Med 77:825–829. https://doi.org/10.1055/s-0030-1250607
17. Sallam MF, Ahmed HMS, El-Nekeety AA, Diab KA, Abdel-Aziem SH, Sharaf HA, Abdel-WahhabMA (2022) Assessment of the oxidative damage and genotoxicity of titanium dioxide nanoparticles and exploring the protective role of holy basil oil nanoemulsions in rats. Biol Trace Elem Res 201:1301–1316. https://doi.org/10.1007/s12011-022-03228-0
18. El-Nekeety AA, Hassan MH, Hassan RR, Elshafey OI, Hamza ZK, Abdel-Aziem SH, Hassan NH, Abdel-Wahhab MA (2021) Nanoencapsulation of basil essential oil alleviates the oxidative stress, genotoxicity and DNA damage in rats exposed to biosynthesized iron nanoparticles. Heliyon 7:e07537. https://doi.org/10.1016/j.heliyon.2021.e07537
19. Quintans-Júnior LJ, Barreto RS, Menezes PP, Almeida JR, Viana AF, Oliveira RC, Oliveira AP, Gelain DP, de Lucca JW, Araújo AA (2013) β-Cyclodextrin-complexed (-)-linalool produces antinociceptive effect superior to that of (-)-linalool in experimental pain protocols. Basic ClinPharmacolToxicol 113:167–172. https://doi.org/10.1111/bcpt.12087
20. Bhalla Y, Jaitak GVK, V, (2013) Anticancer activity of essential oils: a review. J Sci Food Agric 93:3643–3653. https://doi.org/10.1002/jsfa.6267
21. Ta LE, Low PA, Windebank AJ (2009) Mice with cisplatin and oxaliplatin-induced painful neuropathy develop distinct early responses to thermal stimuli. Mol Pain 5:9. https://doi.org/10.1186/1744-8069-5-9
22. Suryani PR, Zulissetiana EF, Prananjaya BA (2019) Antidepressant activity of basil leaves essential oil (Ocimumbasilicum) in male balb/c mice. J Phys Conf Ser 1246(1):012065

23. Ellman GL, Courtney KD, Andres V Jr, Featherstone RM (1961) A new and rapid colorimetric determination of acetylcholinesterase activity. Biochem Pharmacol 7:88–95. https://doi.org/10.1016/0006-2952(61)90145-9
24. Wills ED (1987) Evaluation of lipid peroxidation in lipids and biological membranes. In: Snell K, Mullock B (eds) Biochemical toxicology: a practical approach. IRL Press, Oxford, pp 127–152
25. Aebi H (1984) Catalase in vitro. Meth Enzymol 105:121–126. https://doi.org/10.1016/S0076-6879(84)05016-3
26. Livak KJ, Schmittgen TD (2001) Analysis of relative gene expression data using real-time quantitative PCR and the 2− ΔΔCT method. Methods 25:402–408
27. Abd El-Kareem MSM, Rabbih MAEF, Selim ETM, Elsherbiny EAE, El-Khateeb AY (2016) Application of GC/EIMS in combination with semi-empirical calculations for identification and investigation of some volatile components in basil essential oil. Int J Anal Mass Spectrom Chromatogr 04:14–25. https://doi.org/10.4236/ijamsc.2016.41002
28. Madanagopal P, Ramprabhu N, Jagadeesan R (2022) In silico prediction and structure-based multitargeted molecular docking analysis of selected bioactive compounds against mucormycosis. Bull Natl Res Cent 46:24. https://doi.org/10.1186/s42269-022-00704-4
29. Guex N, Peitsch MC (1997) SWISS-MODEL and the Swiss-PdbViewer: An environment for comparative protein modeling. Electrophoresis 18:2714–2723
30. O'Boyle NM, Banck M, James CA, Morley C, Vandermeersch T, Hutchison GR (2011) Open babel: an open chemical toolbox. J Cheminf 3:33. https://doi.org/10.1186/1758-2946-3-33
31. Biovia DS (2019) Discovery studio visualizer. San Diego
32. Bora KS, Arora S, Shri R (2011) Role of Ocimumbasilicum L. in prevention of ischemia and reperfusion-induced cerebral damage, and motor dysfunctions in mice brain. J Ethnopharmacol. 137(3):1360–5. https://doi.org/10.1016/j.jep.2011.07.066
33. Eberhardt J, Santos-Martins D, Tillack AF, Forli S (2021) AutoDockVina 1.2.0.: new docking methods, expanded force field, and python bindings. J Chem Inf Model
34. Rebehmed J, Alexandre G, Ramanathan S, Agnel Praveen J (2022) Editorial: advances in molecular docking and structure-based modelling. Frontiers in Molecular Biosciences. https://doi.org/10.3389/fmolb.2022.839826
35. Kouassi K, Ganiyou A, Didier D, Benié A, Nahossé Z (2022) In silico docking of rhodanine derivatives and 3D-QSAR study to identify potent prostate cancer inhibitors. Comput Chem 10:19–52. https://doi.org/10.4236/cc.2022.102002
36. Labib MM, Amin MK, Alzohairy AM, Elashtokhy MMA, Samir O, Saleh I, Arif IA, Osman GH, Hassanein SE (2020) In silico targeting, inhibition and analysis of polyketide synthase enzyme in *Aspergillus* ssp. Saudi J BiolSci 27:3187–3198. https://doi.org/10.1016/j.sjbs.2020.10.012
37. Pace A, Giannarelli D, Galiè E, Savarese A, Carpano S, Della Giulia M, Pozzi A, Silvani A, Gaviani P, Scaioli V (2010) Vitamin E neuroprotection for cisplatin neuropathy: a randomized, placebo-controlled trial. Neurology 74:762–766. https://doi.org/10.1212/WNL.0b013e3181d5279e
38. Brouwers EE, Huitema AD, Boogerd W, Beijnen JH, Schellens JH (2009) Persistent neuropathy after treatment with cisplatin and oxaliplatin. Acta Oncol 48:832–841. https://doi.org/10.1080/02841860902806609
39. Quintão NLM, Santin JR, Stoeberl LC, Corrêa TP, Melato J, Costa R (2019) Pharmacological treatment of chemotherapy-induced neuropathic pain: PPARγ agonists as a promising tool. Front Neurosci 13:907. https://doi.org/10.3389/fnins.2019.00907
40. Malik S, Suchal K, Gamad N, Dinda AK, Arya DS, Bhatia J (2015) Telmisartan ameliorates cisplatin-induced nephrotoxicity by inhibiting MAPK mediated inflammation and apoptosis. Eur J Pharmacol 748:54–60. https://doi.org/10.1016/j.ejphar.2014.12.008
41. Zheng JL, Yuan SS, Wu CW, Li WY (2016) Chronic waterborne zinc and cadmium exposures induced different responses towards oxidative stress in the liver of zebrafish. AquatToxicol 177:261–268. https://doi.org/10.1016/j.aquatox.2016.06.001
42. Dodson M, Redmann M, Rajasekaran NS, Darley-Usmar V, Zhang J (2015) KEAP1-NRF2 signalling and autophagy in protection against oxidative and reductive proteotoxicity. Biochem J469:347–355. https://doi.org/10.1042/BJ20150568
43. Zhang C, Xue-Nan L, Li-Run X, Lei Q, Jia L, Jin-Long L (2017) Atrazine triggers hepatic oxidative stress and apoptosis in quails (Coturnix C. coturnix) via blocking Nrf2-mediated defense response. Ecotox Environ Safe 137:49–56. https://doi.org/10.1016/j.ecoenv.2016.11.016
44. Farouk SM, Gad FA, Emam MA (2021) Comparative immuno-modulatory effects of basil and sesame seed oils against diazinon-induced toxicity in rats; a focus on TNF-α immunolocalization. Environ SciPollut Res Int 28:5332–5346. https://doi.org/10.1007/s11356-020-10840-x
45. Seong H, Ryu J, Yoo WS, Kim SJ, Han YS, Park JM, Kang SS, Seo SW (2017) Resveratrol ameliorates retinal ischemia/reperfusion injury in C57BL/6J mice via downregulation of caspase-3. Curr Eye Res 42:1650–1658. https://doi.org/10.1080/02713683.2017.1344713
46. Achkar IW, Abdulrahman N, Al-Sulaiti H, Joseph JM, Uddin S, Mraiche F (2018) Cisplatin based therapy: the role of the mitogen activated protein kinase signaling pathway. J Transl Med 16:96. https://doi.org/10.1186/s12967-018-1471-1
47. Pereira L, Igea A, Canovas B, Dolado I, Nebreda AR (2013) Inhibition of p38 MAPK sensitizes tumour cells to cisplatin-induced apoptosis mediated by reactive oxygen species and JNK. EMBO Mol Med 5:1759–1774. https://doi.org/10.1002/emmm.201302732
48. Rodríguez-García ME, Quiroga AG, Castro J, Ortiz A, Aller P, Mata F (2009) Inhibition of p38-MAPK potentiates cisplatin-induced apoptosis via GSH depletion and increases intracellular drug accumulation in growth-arrested kidney tubular epithelial cells. ToxicolSci 111:413–423. https://doi.org/10.1093/toxsci/kfp145
49. Ayuob NN, Firgany AEL, El-Mansy AA, Ali S (2017) Can Ocimumbasilicum relieve chronic unpredictable mild stress-induced depression in mice? ExpMolPathol 103:153–161. https://doi.org/10.1016/j.yexmp.2017.08.007
50. Poudel R, Stanley JL, Rueda-Clausen CF, Andersson IJ, Sibley CP, Davidge ST, Baker PN (2013) Effects of resveratrol in pregnancy using murine models with reduced blood supply to the uterus. PLoS One 8:e64401. https://doi.org/10.1371/journal.pone.0064401
51. Rice-Evans CA, Miller NJ, Paganga G (1996) Structure-antioxidant activity relationships of flavonoids and phenolic acids. Free RadicBiol Med 20:933–956. https://doi.org/10.1016/0891-5849(95)02227-9
52. Owoeye O, Isaac AA, Ebenezer OF (2018) Pretreatment with taurine prevented brain injury and exploratory behaviour associated with administration of anticancer drug cisplatin in rats. Biomed Pharmacother 102:375–384. https://doi.org/10.1016/j.biopha.2018.03.051
53. Bhavya ML, Chandu AGS, Devi SS (2018) Ocimumtenuiflorum oil, a potential insecticide against rice weevil with anti-acetylcholinesterase activity. Ind Crops Prod 126:434–439. https://doi.org/10.1016/j.indcrop.2018.10.043
54. Kaplan SV, Limbocker RA, Gehringer RC, Divis JL, Osterhaus GL, Newby MD, Sofis MJ, Jarmolowicz DP, Newman BD, Mathews TA, Johnson MA (2016) Impaired brain dopamine and serotonin release and uptake in wistar rats following treatment with carboplatin. ACS Chem Neurosci 15:689–99. https://doi.org/10.1021/acschemneuro.5b00029
55. Sentari M, Harahap U, Sapiie TWA, Ritarwan K (2019) Blood cortisol level and blood serotonin level in depression mice with basil leaf essential oil treatment. Maced J Med Sci 30:2652–2655. https://doi.org/10.3889/oamjms.2019.819
56. Satou T, Kasuya H, Maeda K, Koike K (2014) Daily inhalation of α-pinene in mice: effects on behavior and organ accumulation. Phytother Res 28:1284–1287. https://doi.org/10.1002/ptr.5105
57. Fatriansyah JF, Rizqillah RK, Yandi MY, Fadilah Sahlan M (2022) Molecular docking and dynamics studies on propolissulabiroin-A as a potential inhibitor of SARS-CoV-2. J King Saud Univ Sci 34:101707. https://doi.org/10.1016/j.jksus.2021.101707
58. Prajapati P, Jaya P, Poonam T, Kirti S, Manishkumar R (2022) Molecular structural, hydrogen bonding interactions, and chemical reactivity studies of ezetimibe-l-prolinecocrystal using spectroscopic and quantum chemical approach. Front Chem 15:848014. https://doi.org/10.3389/fchem.2022.848014

Publisher's Note